

Improved search of PCA databases for spectro-polarimetric inversion

R. Casini,^a A. Asensio Ramos,^b B. W. Lites,^a A. López Ariste^c

^a*High Altitude Observatory, National Center for Atmospheric Research,¹
P. O. Box 3000, 80307-3000, Boulder, CO, U.S.A.*

^b*Instituto de Astrofísica de Canarias, c/ Vía Láctea s/n, E-38205 La Laguna, Tenerife, Spain*

^c*THEMIS, CNRS UPS 853, c/ Vía Láctea s/n, E-38200 La Laguna, Tenerife, Spain*

ABSTRACT

We describe a simple technique for the acceleration of spectro-polarimetric inversions based on principal component analysis (PCA) of Stokes profiles. This technique involves the indexing of the database models based on the sign of the projections (PCA coefficients) of the first few relevant orders of principal components of the four Stokes parameters. In this way, each model in the database can be attributed a distinctive binary number of 2^{4n} bits, where n is the number of PCA orders used for the indexing. Each of these binary numbers (indexes) identifies a group of “compatible” models for the inversion of a given set of observed Stokes profiles sharing the same index. The complete set of the binary numbers so constructed evidently determines a partition of the database. The search of the database for the PCA inversion of spectro-polarimetric data can profit greatly from this indexing. In practical cases it becomes possible to approach the ideal acceleration factor of 2^{4n} as compared to the systematic search of a non-indexed database for a traditional PCA inversion. This indexing method relies on the existence of a physical meaning in the sign of the PCA coefficients of a model. For this reason, the presence of model ambiguities and of spectro-polarimetric noise in the observations limits in practice the number n of relevant PCA orders that can be used for the indexing.

1. Introduction

One of the biggest challenges that the astronomical community faces with the next generation of astronomical instrumentation, both ground based and space borne, is without doubt the enormous amount of data that will need to be stored, reduced, analyzed, and finally interpreted in terms of physical processes. This problem is particularly striking in the case of solar observations, where essentially every pixel of the detector contributes to the science data. As an example, the expected volume of spectro-polarimetric data that will be produced by the Advanced Technology Solar Telescope (Rimmele et al. 2008) is of the order of 16 TB per day.

¹The National Center for Atmospheric Research is sponsored by the National Science Foundation.

The inversion of spectro-polarimetric data is by itself a notoriously challenging problem of solar physics. This is because the emergence of a polarized signal in the solar spectrum, starting from a fundamentally isotropic (and hence, unpolarized) radiation within the solar interior, can only be explained through a complicated description of the interaction of light with a gas of ions in a temperature and pressure stratified atmosphere, and in the presence of magnetic fields that are often entangled down to and below the smallest spatial scales observable with present-day instrumentation. For this reason, the inversion of spectro-polarimetric signals is intrinsically an ill-posed problem, and the forward modeling of the polarized solar spectrum can be very time consuming, depending on the type of spectral lines considered, and on where these lines form on the Sun (Trujillo Bueno 2010; Casini 2012).

The development of time-efficient inversion techniques for spectro-polarimetric data is a thriving field of research in solar physics. We will not discuss here the merits and issues of the various approaches to spectro-polarimetric inversion, and we refer instead the reader to a review by Asensio Ramos (2012) for such a discussion. Here we want to focus on the problematics associated with inversion methods that rely on pattern-recognition techniques, and more specifically, *principal component analysis* (PCA; Pearson 1901; Jolliffe 2002), which has successfully been applied to spectro-polarimetric observations of the solar photosphere (Rees et al. 2000), and of solar prominences and filaments (López Ariste & Casini 2003; Casini et al. 2003; Casini, Bevilacqua, & López Ariste 2005; Kuckein et al. 2009).

In the next section we briefly summarize the ideas behind PCA-based inversion of spectro-polarimetric data (see also, Rees et al. 2000; Skumanich & López Ariste 2002; López Ariste & Casini 2002). In Section 3, we present our idea for the indexing of the inversion database, its justification, and its limits of applicability. Finally, in Section 4, we present some test results of PCA inversions with indexed databases, applied to on-disk observations of He I 1083 nm that were performed by one of us (B.L.). We provide an outlook for further development in our concluding remarks.

2. Principal Component Analysis

We briefly summarize below the basic concepts of PCA Stokes inversion, for the sake of completeness, and also for introducing notation essential to this study.

We consider the case of a spectrally and spatially resolved observation of a solar region with a spectro-polarimeter. This observation is fully characterized by the set of Stokes vectors $\mathbf{S}_j(\lambda_i) \equiv (I_j(\lambda_i), Q_j(\lambda_i), U_j(\lambda_i), V_j(\lambda_i))$, where $i = 1, \dots, N$ indicates the wavelength points sampled by the spectro-polarimeter, and $j = 1, \dots, M$ indicates the spatially resolved elements of the observed region. In the Stokes notation, I refers to the light intensity, Q and U are the two independent states of linear polarization on the plane normal to the direction of light propagation, and V is the Stokes parameter for circular polarization around that direction. Let us indicate with S any of the four Stokes parameters, I , Q , U , and V . Then the spectro-polarimetric observation of the solar

region *for that parameter* naturally define the $N \times M$ matrix

$$\mathbf{S}_{ij} = S_j(\lambda_i), \quad i = 1, \dots, N; \quad j = 1, \dots, M. \quad (1)$$

The M observed points in the solar region form a set of statistically independent realizations of the Stokes profile $S(\lambda)$. We can then calculate the averages

$$\bar{S}(\lambda_i) = \frac{1}{M} \sum_{j=1}^M \mathbf{S}_{ij}, \quad i = 1, \dots, N, \quad (2)$$

for each of the wavelength points, and the $N \times N$ *covariance* matrix

$$\mathbf{C}_{ij} = \sum_{l=1}^M [\mathbf{S}_{il} - \bar{S}(\lambda_i)][\mathbf{S}_{jl} - \bar{S}(\lambda_j)], \quad i, j = 1, \dots, N. \quad (3)$$

This is a real and symmetric matrix, which therefore can always be diagonalized by an orthogonal transformation (e.g., Birkhoff & Mac Lane 1953). The solution of the corresponding eigenvalue problem,

$$\mathbf{C}\mathbf{f}^{(k)} = e^{(k)}\mathbf{f}^{(k)}, \quad k = 1, \dots, N, \quad (4)$$

is known to provide an optimal set of orthogonal *eigenprofiles* – represented by the N -dimensional eigenvectors $\mathbf{f}^{(k)}$ – for the decomposition of the residual signals $S_j(\lambda) - \bar{S}(\lambda)$ (Jolliffe 2002). These eigenprofiles are also known as the *principal components* of the observed set of profiles. Another property of the covariance matrix is to be positive semidefinite (e.g., Jolliffe 2002), hence $e^{(k)} \geq 0$, for all k . In particular, solving the eigenvalue problem (4) by singular value decomposition (SVD; e.g., Press et al. 2007) provides us with an ordered set of eigenprofiles according to the decreasing non-negative amplitude of the corresponding singular values. This ordering reflects the importance of the contribution of the various eigenprofiles to the covariance of the observations.

The eigenprofiles $\mathbf{f}^{(k)}$ form a basis for the space of the residual signals $S_j(\lambda) - \bar{S}(\lambda)$. In particular, this implies that the j -th profile in the set of M observations can be reconstructed *exactly* from its set of *PCA components*,

$$c_j^{(k)} \equiv \sum_{i=1}^N \mathbf{f}_i^{(k)} [\mathbf{S}_{ij} - \bar{S}(\lambda_i)], \quad k = 1, \dots, N, \quad (5)$$

so that

$$S_j(\lambda) - \bar{S}(\lambda) \doteq \sum_{k=1}^N c_j^{(k)} \mathbf{f}^{(k)}. \quad (6)$$

When the eigenprofiles $\mathbf{f}^{(k)}$ are ordered according to their corresponding singular values, then any truncation of the summation in Equation (6) provides an approximation of the residual $S_j(\lambda) - \bar{S}(\lambda)$. It is found in practice that a small number n of eigenprofiles ($n \sim 10$) is often sufficient to reconstruct the residual signals within the typical polarimetric noise of the observations.

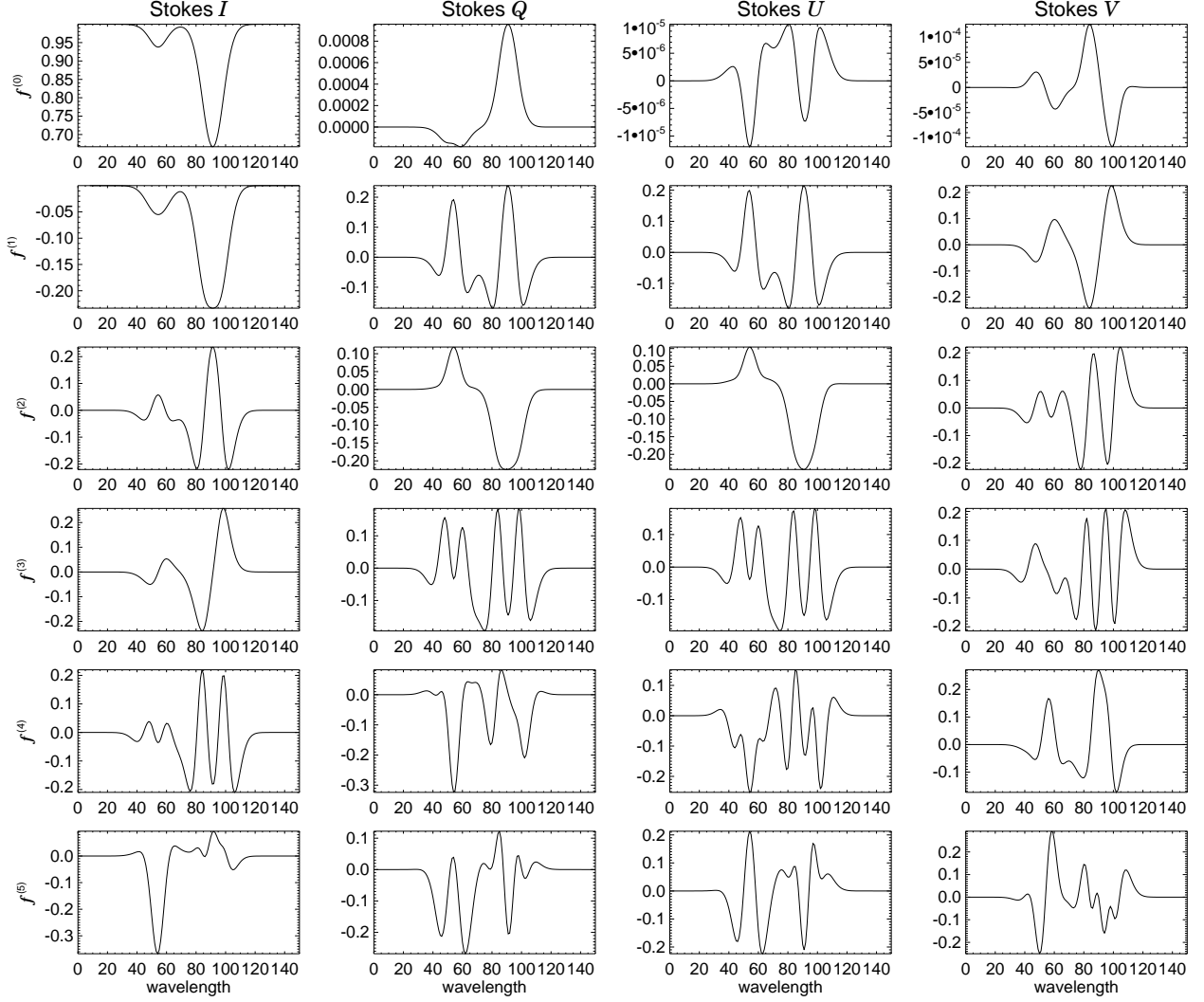


Fig. 1.— The average profiles (top row) and the first five PCA eigenprofiles (next five rows) for each of the four Stokes parameters, I , Q , U , and V (columns), extracted from a database of synthetic Stokes profiles of the He I chromospheric lines at 1083 nm. The rows correspond to increasing orders of the eigenprofiles, with $f^{(0)} = \bar{S}(\lambda)$. The forward model used in the derivation of this eigenbasis corresponds to on-disk observations of the He I lines, for inclinations of the line of sight to the local normal to the surface between 30° and 40° . The database comprises all possible orientations of the magnetic field vector (i.e., $0 \leq \vartheta_B \leq \pi$ and $-\pi \leq \varphi_B \leq \pi$), and magnetic strengths between 0.2 and 2000 G logarithmically sampled. The calculated profiles emerge from a homogenous slab of plasma with optical depth at line center between 0.1 and 1.5, and temperature between 5000 and 25,000 K. The position height of the slab (which affects the radiation anisotropy) varies between 0 and $0.06 R_\odot$. Bulk velocities are accounted for by randomly displacing the rest frequency of each model within a pixel unit of Doppler shift. Because of the homogenous slab assumption, velocity gradients are not taken into account.

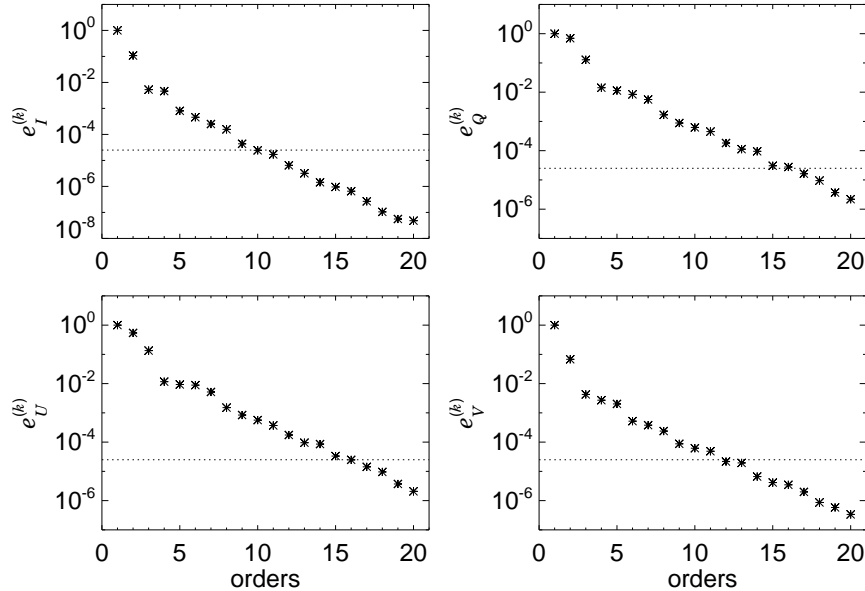


Fig. 2.— Amplitudes of the first 20 singular values corresponding to the basis of eigenprofiles partially shown in Figure 1, for the four Stokes parameters, I , Q , U , and V . For each plot, the displayed values were normalized to the value for $k = 1$. These amplitudes estimate the covariance of the model Stokes profiles along the “principal directions” represented by the eigenprofiles. The dotted lines show a threshold of 2.5×10^{-5} , which corresponds approximately to an error of 10^{-3} in the reconstruction of a synthetic profile (see text).

For the inversion of spectro-polarimetric data we must rely on a model of the magnetized atmosphere that describes the line formation region. Thus it is often preferable to determine the eigenprofiles $\mathbf{f}^{(k)}$ from a database of synthetic line profiles based on the model assumptions, rather than from the actual observations. Since they come from a model, these profiles are generally noiseless. Figure 1 show the first five eigenprofiles plus the average profile, for each of Stokes I , Q , U , and V , for the multiplet of He I at 1083 nm observed on the disk. The figure caption lists the ranges of the physical parameters for the model adopted for the synthesis. This model is the same as the one used for the inversion tests presented in Section 4. The set of synthetic profiles from which this eigenbasis is extracted consists of 50,000 models spanning the parameter space. In order to improve the sampling “efficiency” of such a limited number of models, we adopted the *Latin Hypercube Sampling* variant of the Monte Carlo method (McKay, Beckman, & Conover 1979) for the construction of this set.

Figure 2 demonstrates instead the drop-off of the singular values of the covariance matrix (3) for the first 20 eigenprofiles. The relative magnitude of these singular values estimates the model’s covariance along any of the “principal directions” in the N -dimensional space spanned by the eigenprofiles. From Figure 1 we see that the peak amplitude of the eigenprofiles is typically around 0.2. Thus, for a polarimetric noise of 10^{-3} , we expect to be sensitive to profile covariances of

the order of $(10^{-3}/0.2)^2 = 2.5 \times 10^{-5}$, which is indicated in Figure 2 by the dotted line. From that figure, taking also into account the local drop-off of the covariances around the specified threshold, we can conclude that, for the purpose of Stokes profile reconstruction and inversion, we should retain approximately 11 orders for Stokes I , 14 for Q and U , and 13 for V . These numbers must be compared with the dimension N of the complete set of eigenprofiles in the database, which corresponds to the number of wavelength points (in this case, $N = 151$) used for the synthesis of the Stokes profiles. As a result, the description of the Stokes profiles for our model in terms of their principal components allows a data compression of the spectro-polarimetric information by approximately a factor 10.

It is important to observe that the above argument about the number of orders that must be retained for spectro-polarimetric inversions relies on two fundamental assumptions. The first assumption is that the error bars of the profiles are dominated by photon noise, and the second one that the photon counts is large enough that the associated poissonian noise can be treated as a random variate, so that its variance can simply be added to that of the model. On the other hand, the systematic errors due to deviations of the observations from the line formation model, especially in the case of complicated atmospheric structures, is very likely to dominate the inversion errors. Thus, in practical cases, we should not expect that retaining such a high number of orders necessarily improves the goodness of the profile fits from the inversion. We will come back to this argument in the next section.

3. Indexing of PCA inversion databases

We created an inversion database of 0.75 million models spanning the same parameter space as the eigenbasis of Figure 1. The profile information in this database is encoded in the expansion coefficients given by Equation (5). The inversion database is constructed by a strategy of “filtered” Monte Carlo sampling, where each new randomly selected point in the parameter space is tested for proximity to previously included models in the database. The testing parameter is the *PCA distance* between two models, i and j , which is defined as follows, for each of the four Stokes parameters:

$$d_{ij} = \left(\sum_{k=1}^m [c_i^{(k)} - c_j^{(k)}]^2 \right)^{1/2}, \quad (7)$$

where m is the maximum number of orders retained for the reconstruction of the Stokes profiles. The filtering criterion is to reject models for which the cumulative PCA distance for the four Stokes parameters² is less than a predefined value, δ . The value of δ is reduced (increased) during the construction of the database when the rejection rate of new models becomes too large (small).

²This cumulative distance can be defined in several different ways. Its specific form is not essential for the following discussion.

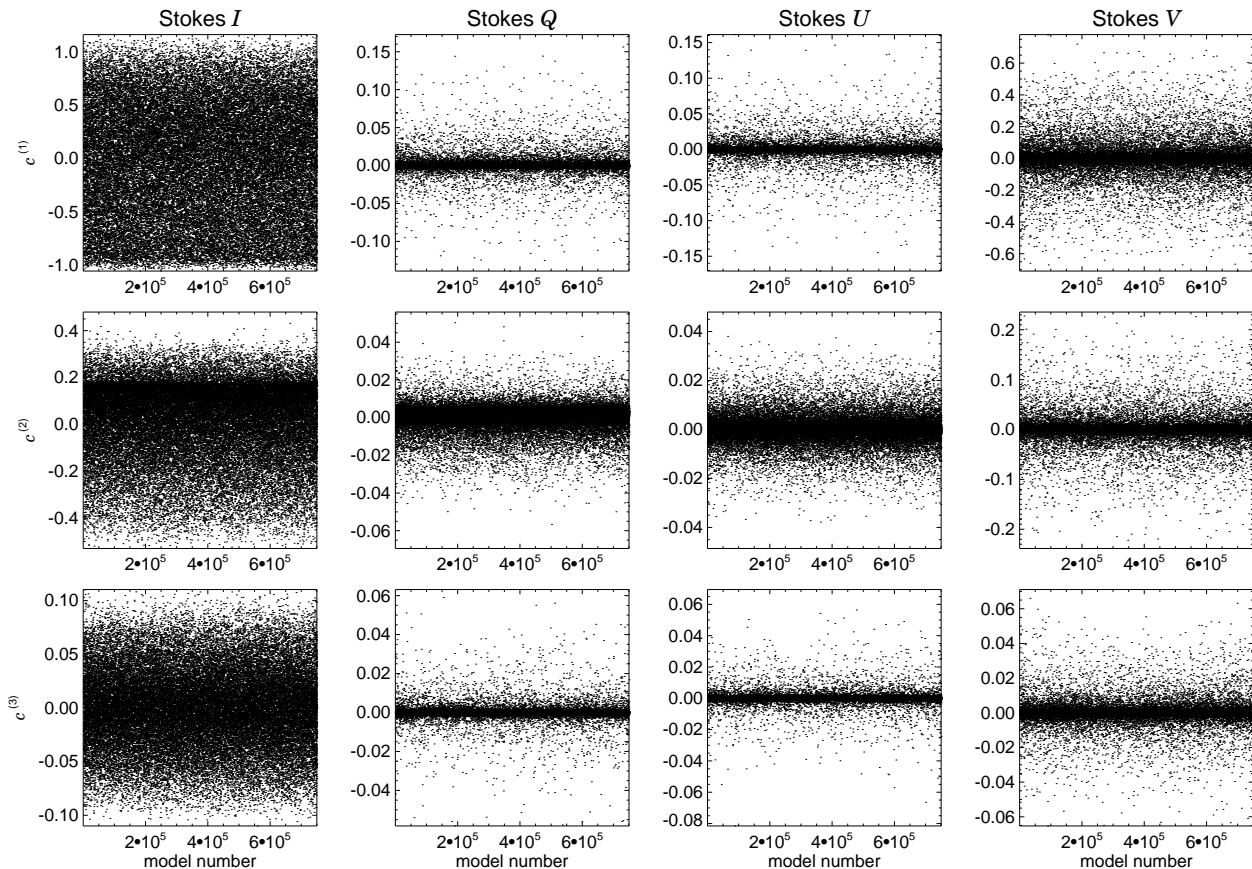


Fig. 3.— Scatter plots of the PCA coefficients for the atmospheric model considered in Figure 1. Only the first three orders of eigenprofiles (rows) for each of the four Stokes parameters, I , Q , U , and V (columns), are shown. These plots span the entire inversion database, with a total of 0.75 million models. (For plotting convenience, here we only show one every fifteen points in the database.) We note the clear tendency for the PCA coefficients to be distributed rather evenly around a zero average.

This strategy allows to build up large-size databases where the shapes and amplitudes of the Stokes profiles are homogeneously distributed.

Because of the Monte Carlo construction of the inversion database, the distribution of the models in the database is completely random. Thus the PCA inversion ordinarily requires a full search through the database in order to identify the closest model (in terms of PCA distance) to the observations, and this search must be repeated for each of the observed set of Stokes profiles. For complicated atmospheric models, which may depend on many parameters, the number of models in the database that is needed for an accurate PCA inversion can be in the order of millions. The systematic search of such large databases represents one of the most critical downsides of inversion methods based on pattern-recognition techniques. It is thus important to devise ordering strategies

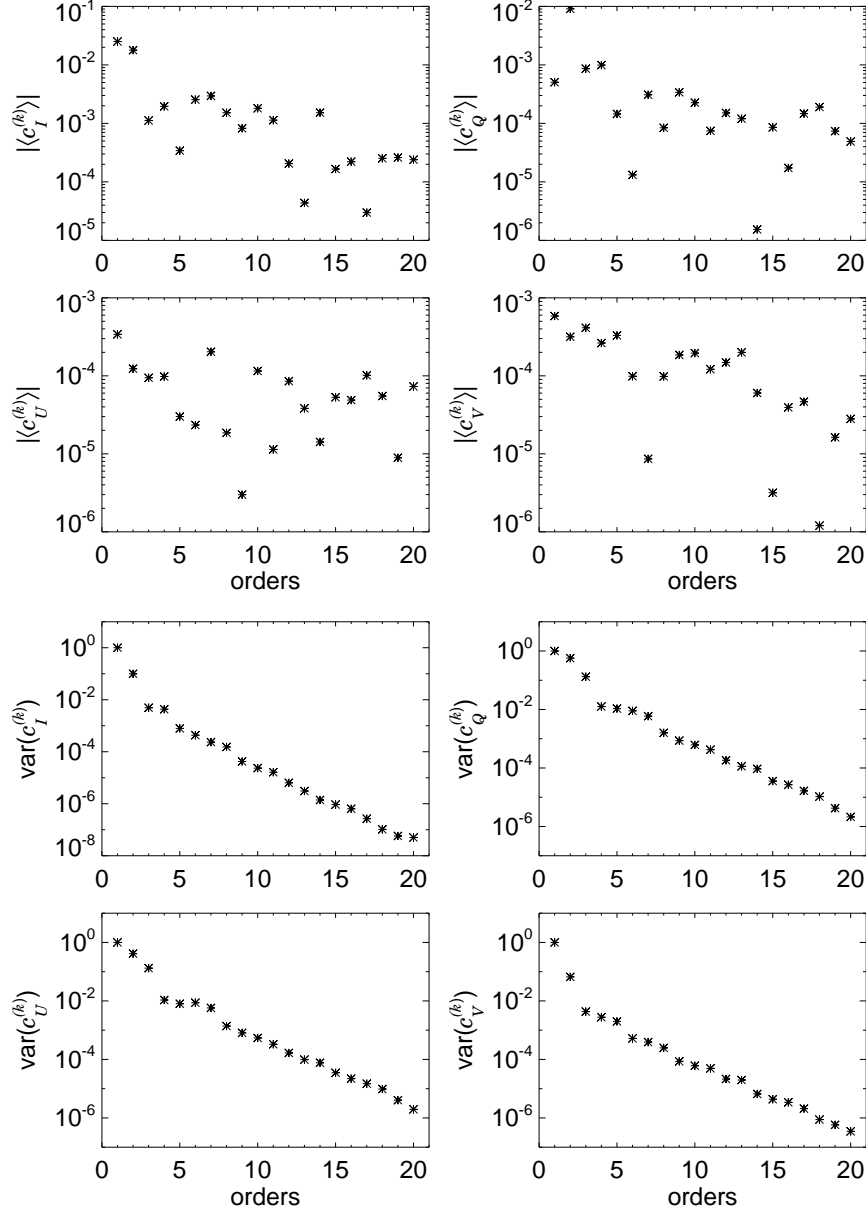


Fig. 4.— Amplitudes of the absolute mean (top) and variance (bottom) of the first 20 PCA coefficients for the four Stokes parameters, I , Q , U , and V , calculated over the same 50,000 models of the inversion database as for the case of Figure 3. For each Stokes parameter and order k , the mean value of the PCA coefficient was normalized to its maximum absolute value within the database. The first three points in each plot correspond then to the (normalized) mean values of the distributions shown in Figure 3. These plots confirm the fact that the PCA coefficients tend to be approximately distributed around zero. The variance values were instead normalized to the value for $k = 1$. As expected, the variance plots are practically identical to the plots of the singular values of the covariance matrix, given in Figure 2.

for the inversion databases that can significantly reduce the search time.

The strategy that we propose in this work relies on the characteristic distribution of the values of the PCA coefficients $c_i^{(k)}$ within the inversion database, for each of the four Stokes parameters. This distribution, for the atmospheric model and inversion database considered in this work, is presented in Figure 3, for $k = 1, 2, 3$, and for the first 50,000 models of the database. We note immediately the tendency for the PCA coefficients to be distributed rather evenly around a zero average (see also Figure 4). This is largely a consequence of the fact that the average Stokes profiles are subtracted out for the definition of the covariance matrix, Equation (3). Since the low-order eigenprofiles contribute more importantly to the reconstructed profiles (see the variance plots of Figure 4, as well as Figure 2), we can expect that the *sign* of the PCA coefficients for these orders will also be important in determining the shape and amplitude of the Stokes profiles that must be matched to the observations. In other words, we can make the assumption that, *in comparing models with observations, the signs of the corresponding PCA coefficients for the lowest orders must match.*

Based on this assumption, we can partition the inversion database into disjoint classes, each of them being characterized by a unique string of signs characterizing the PCA coefficients of the models in that class. In particular, we may convene to attribute the value 0 to “–” and the value 1 to “+”, in which case each of these classes are identified by a unique binary number. Since there are four Stokes parameters, each PCA order gets associated with a 4-bit number, and the number of classes that each order brings to the partitioning corresponds to the number of integers that can be built with a 4-bit number, i.e., $2^4 = 16$. The total number of classes of the database partition is thus 2^{4n} , where n is the number of orders used for the indexing. The resulting partition classes can then be ordered according to the increasing value of the binary index number associated with each class. If one class corresponds to a string of signs that have no match within the database, then that particular class will be empty. This indexing of the database models allows to access directly the desired class for the inversion. In practice, one determines the indexing number from the PCA coefficients of the observations, and then looks for the best matching model in the database by restricting the search to the class with the same index.

Typically, the order of indexing, n , will be a small number, say, between 1 and 3. There are essentially two reasons for this. First of all, a high level of partitioning could make the number of models in each class too small, depending on the total number of models in the database, thus affecting the statistical significance of the inversion. Secondly, because the amplitude of the PCA coefficients decreases rather rapidly with the order number (see variance plots of Figure 4), the signs of high-order coefficients *for the observations* could largely be affected by noise as well as other systematic errors.

We already hinted to this problem at the end of the previous section. However, through the variance plots of Figure 4 we can better assess the relative significance of the high-order eigenprofiles for Stokes inversion. In fact, we can imagine to produce similar variance plots for the PCA

coefficients of the decomposition of the observed data into their principal components. If the line formation model were representative of the observations, we should then expect that the variance plots for the observations and the database would be similar. In contrast, the presence of systematic effects in the observations, not accounted for by the model, would be demonstrated by a deviation between the two sets of variance curves, respectively, for the observations and the model. Typically, the two sets of variance curves will overlap for the very first PCA orders, and then start diverging from some order k_0 on. It then becomes meaningless – and, in fact, even detrimental – to retain any PCA order larger than k_0 for the inversion.

We can therefore conclude that high orders should not be trusted for the purpose of preselecting inversion classes within the database. This conclusion is supported also by the fact that the relative number of empty classes within the database is empirically found to increase with the number of orders used for the indexing. So there is an increased risk that an observed set of Stokes profiles, perhaps because of unknown systematic effects in the formation of the spectral line affecting one of these high-order signs, be matched to an empty class of the database and not be inverted.

Of course, it is possible to devise alternative strategies for the indexing of the inversion database. For example, in a study of the PCA inversion of the photospheric lines of Fe I at 630 nm observed in active regions, Eydenberg, Balasubramaniam, & López Ariste (2005) partitioned the inversion database into three subsets, corresponding to the three distinct magnetic regions of sunspot umbra, sunspot penumbra, and quiet Sun. The characteristic magnetic fields and thermodynamics of those three photospheric regions allowed the computation of synthetic profiles using correspondingly different sets of model parameters and eigenprofiles. In that work, the purpose of the authors was not directly to improve the inversion speed, but rather to attain a denser covering of the parameter space for each of the identified photospheric regions, in order to improve the quality of interpolate inversions.

In our work, we focused instead on the distribution of the Stokes profiles’ shapes as characterized by the distribution of the PCA coefficients within the database, rather than on the physical characteristics of the emitting solar region (although these two viewpoints are evidently correlated). The proposed method of database partitioning is obviously the simplest that can be devised, as it relies only on the assumption that the PCA coefficients’ mean gathers around zero. This assumption is well justified, for the particular line formation model of the He I 1083 nm that we considered in this work, but it may not always be the case for other line formation models, for example, in a database created for near-limb data, where on-disk absorption profiles and off-limb emission profiles may be mixed within the database. Indeed, already in the database we considered for this work, we can notice some visible deviation from zero mean, as well as some skewness, in the distributions of the first two PCA coefficients for Stokes I (see Figure 3). Our method could then be immediately generalized by adopting instead the true mean of a PCA coefficient’s distribution, or otherwise its median. In particular, using the median would guarantee a better balanced population of the partition classes, with two immediate advantages: (1) overall improvement of the statistical significance of the indexed inversions, and (2) approaching of the increase factor of the inversion speed to the

indexing	reading time	inversion time
none	36 s	730 s
1st-order (16 classes)	38 s	50 s (0)
2nd-order (256 classes)	38 s	6 s (0)

Table 1: Inversion times for the magnetic maps of Figure 5, for three different orders of indexing of the PCA inversion database using 0.5 million models out of the total 0.75 million in the database. Each inversion was run as a single thread on a processor Intel Quad Core i7 2.2 GHz. The increase factors of the inversion speed for the two cases of indexed databases are approximately 15 and 120, respectively. The number between parentheses next to the inversion time represents the number of non-inverted points in the map for the indexed inversion. The reading time is the overhead time necessary to read in the database and store its information in the computer memory for the inversion.

theoretical maximum of 2^{4n} . A further improvement of the indexing strategy for PCA databases would be to look at higher-order moments of the coefficient distributions, such as the variance. This information could be used to define a new partition class of models, where the distance of a given PCA coefficient from the mean is less than some prescribed fraction of a standard deviation. With this type of partitioning, the number of classes becomes 3^{4n} , and so one can attain a reduction of the inversion time by two orders of magnitude already for $n = 1$.

4. Test results and discussion

We tested the proposed method of indexing of the PCA inversion database to a set of He I 1083 nm observations performed by one of the authors (B.L.) with the Tenerife Infrared Polarimeter II instrument (TIP II; Collados et al. 2007) deployed at the German Vacuum Tower Telescope (VTT, Tenerife, Spain). These observations were performed on NOAA Active Region 11259 (406 arcsec east, 334 arcsec north of disk center) on 22 July, 2011 between 07:31 and 08:24 UT, with full Stokes spectral imaging of the region around the He I 1083 nm lines from TIP II, plus imaging of the spectral region around the Ca II lines at 854.2 nm in Stokes *I* only with the VTT spectrograph. Atmospheric seeing was very good during these observations, and the image quality was enhanced by usage of the KAOS adaptive optics system. Here we discuss only the observations of the He I lines. The spectral sampling of the TIP II data was 0.0109 Å/pixel, spanning a spectral region of 11 Å around the He I lines including the Si I line at 1082.7 nm. Along the slit dimension (solar N-S) the sampling was 0.175 arcsec, spanning 78 arcsec. At each of the 240 scan positions (from solar E to W) of the spectrograph slit the signal was integrated for 10 seconds. During data reduction the data were re-binned by a factor of 3 in wavelength, a factor of 5 along the slit, and a factor of 3 in the slit scan direction in order to increase the signal-to-noise ratio (S/N) for the weak Stokes polarization signals. The data subjected to this analysis has 336 wavelength steps of 0.0328 Å, 89 positions along the slit of spacing 0.875 arcsec, and 80 positions in the slit scan

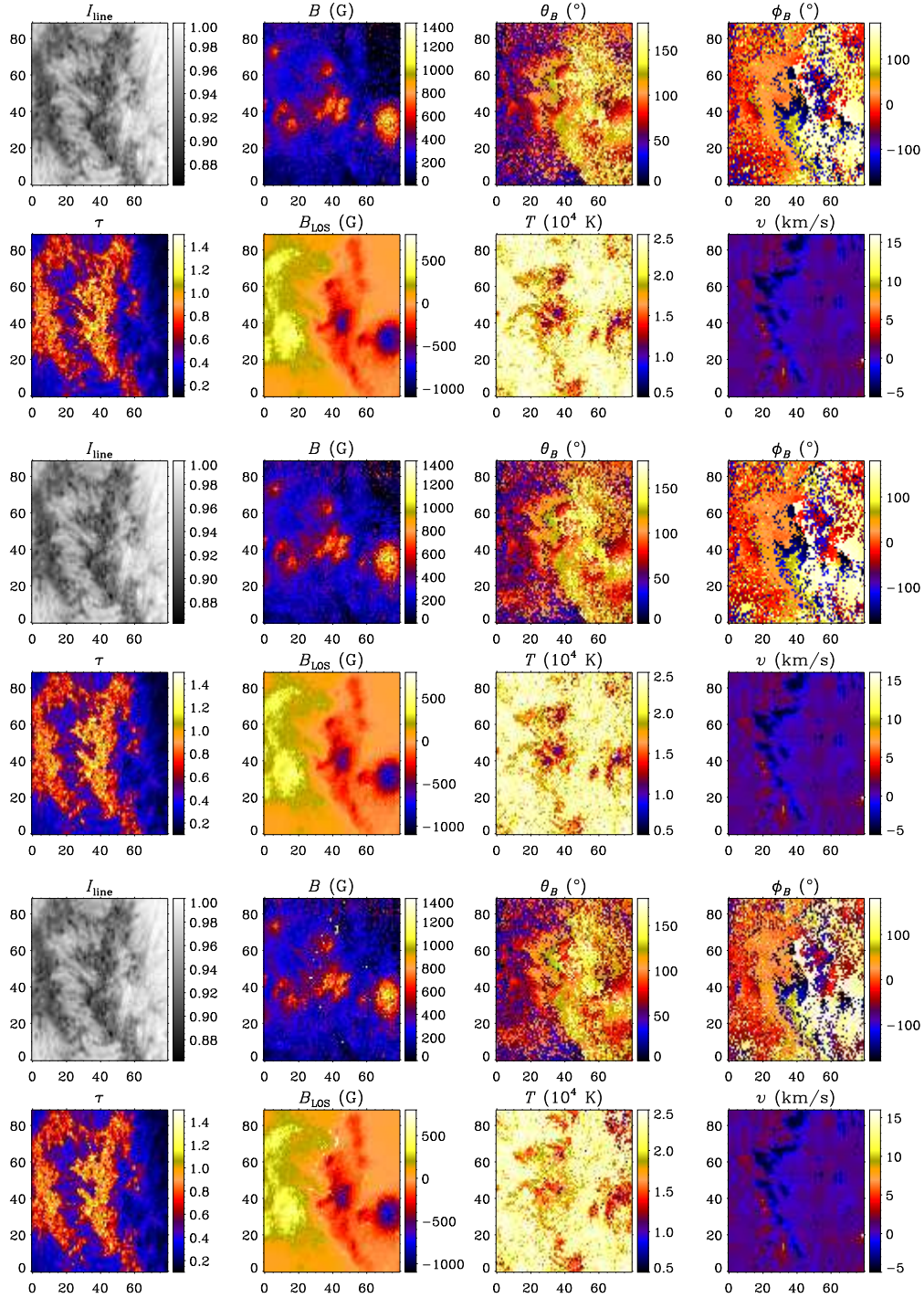


Fig. 5.— Magnetic maps for the dataset described in the text, corresponding to inversions run with the original non-indexed database (top), and with indexed databases through the first order (16 partitions; middle) and second order (256 partitions; bottom) of eigenprofiles. See the text for a description of the inverted quantities.

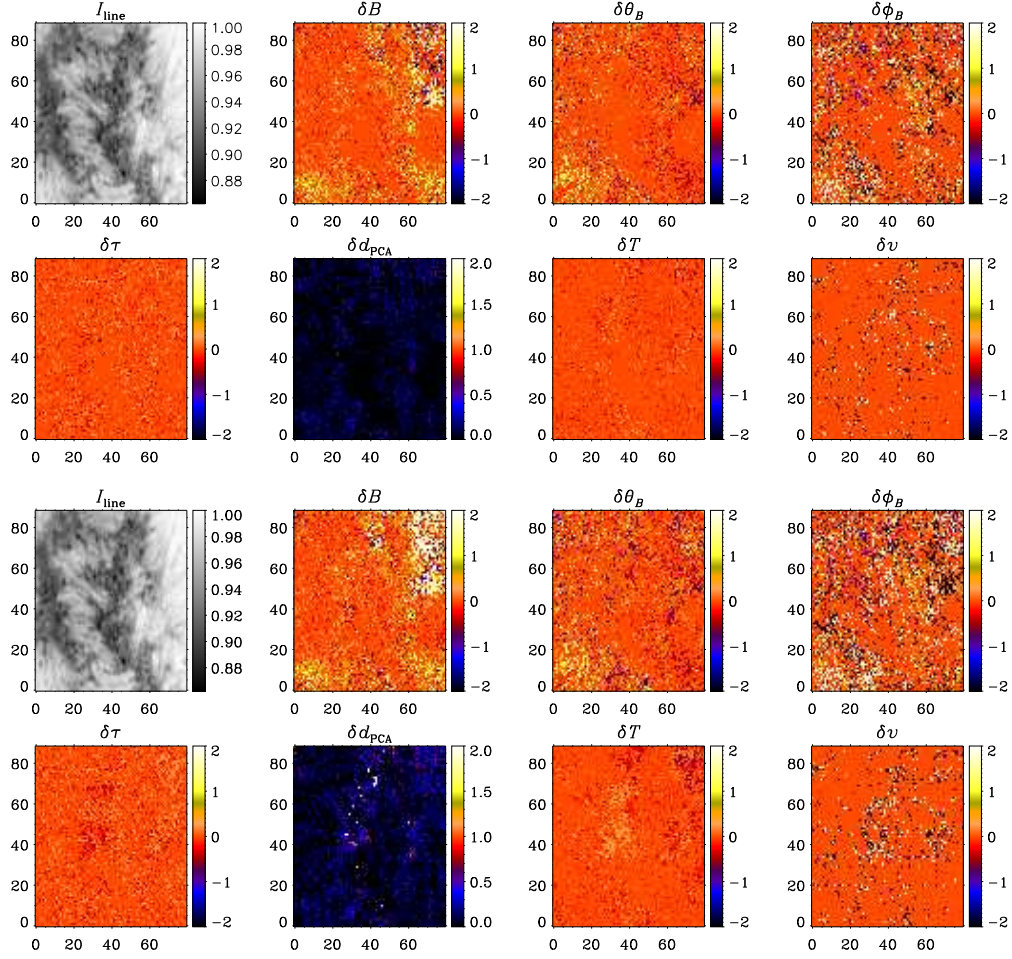


Fig. 6.— Difference maps for the indexed inversion of 1st (top) and 2nd order (bottom), relative to the inversion with the non-indexed database. For each inverted parameter, p , these maps show the relative difference $\delta p \equiv 2(p^{(k)} - p^{(0)})/(|p^{(k)}| + |p^{(0)}|)$, where k is the indexing order of the inversion database.

direction of 1.05 arcsec. The resulting S/N as determined empirically from the r.m.s. fluctuation in the polarization continua is 0.024%, 0.018%, and 0.028%, respectively for Q , U , and V . The spectral range of these observations extends well beyond the blue and red wings of He I 1083 nm. As demonstrated by the Stokes eigenprofiles of Figure 1, the 151 wavelength points adopted for the PCA database are sufficient to encompass the spectral range of the multiplet.

We inverted all 7120 pixels in the map, first with the original database of 0.75 million models, and then with the same database indexed according to the proposed strategy, using $n = 1$ (16 partition classes) and $n = 2$ (256 partition classes). Following the argument given in the previous section, with regard to the maximum number k_0 of orders to retain for the inversion, the set of variance plots produced for the observed data indicated that we should use 4 eigenprofiles for

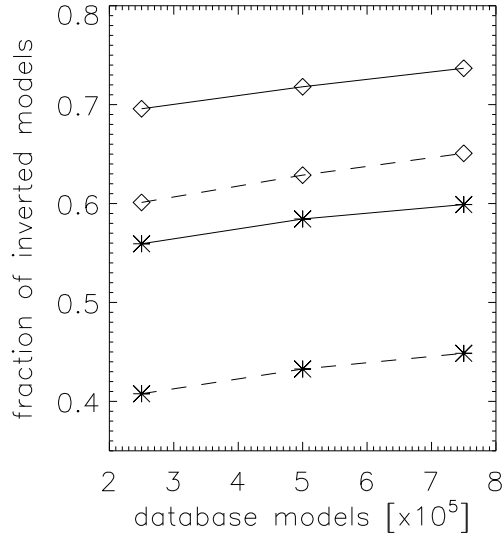


Fig. 7.— Plots of the percentage of inverted models whose properties are preserved in passing from a non-indexed to an indexed inversion: ($*$) all physical parameters of the models are preserved; (\diamond) the inverted magnetic strength varies by less than 20%. The continuous (dashed) lines correspond to the indexed inversions of order 1 (2).

Stokes I , and 3 for all of Stokes Q , U , and V . The magnetic maps resulting from these inversions are displayed in Figure 5. The inversion times for the three tests are given in Table 1.

The inversion results shown in Figure 5 are presented in the form of “magnetic maps”, each consisting of eight panels. These, from left to right and top to bottom, give the line-center intensity map of the observed region, the magnetic field strength in gauss, the magnetic field vector inclination from the local vertical, and its azimuth counted counterclockwise from the direction defined by the projected solar radius through the observed point (not showing in these maps), the line-center optical depth of the slab from which the line’s Stokes profiles emerge, the longitudinal component of the magnetic field, the plasma temperature as defined by the line’s Doppler width, and finally the line-of-sight velocity as determined by the line’s Doppler shift, where the zero reference is given by the line position averaged over the entire map.

The differences introduced in the inversion by the indexing of the PCA database are shown in Figure 6, for both orders of indexing. In those maps, the B_{LOS} panel has been replaced by the relative increase of the PCA distance, which estimates the goodness of the inversion. Because of the introduction of disjoint classes in the database, we must expect that the PCA distance can only increase (hence, leading to an overall worse fitting of the observations), with respect to the case where the PCA database is not indexed. For each of the inverted parameters, p , the maps of Figure 6 give the relative difference $\delta p \equiv 2(p^{(k)} - p^{(0)})/(|p^{(k)}| + |p^{(0)}|)$, where k is the indexing order of the PCA database used for the inversion. These maps show that the results for the indexed inversion of order 1 (2) are exactly identical to those for the non-indexed inversion only for 59.9%

(44.9%) of the inverted points. As an example of the changes produced by the indexing of the PCA database, we consider the case of the magnetic field strength. This is found to change by less than 20% over 73.7% (65.1%) of the observed region, for the indexed inversion of order 1 (2). (See also Fig. 7).

We notice, however, that the largest relative errors on the inverted field strength, with variations in excess of 100%, tend to occur in regions of the map where the inferred magnetic field is very small (cf. maps in Figure 5). This is a direct consequence of our definition of the relative error δp given above. While this definition was adopted so to prevent the inversion error from diverging in some points of the map, it is evident that large errors can still be expected for small values of $p^{(0)}$, with a theoretical maximum of 200% (cf. maps in Figure 6) when $p^{(0)}$ vanishes. We also observe that several points along the magnetic neutral line suffer a noticeable increase of the error in the inferred magnetic strength for the order 2 of database indexing. While the number of such points is by no means statistically significant, it is easy to provide an interpretation of this result. Along the neutral line, we expect that the PCA coefficients associated with Stokes V will be very close to zero, and therefore the signs of those coefficients, which determine the specific indexing class of those profiles, loses significance. Reliance on the sign of those coefficients is therefore bound to increase the inversion error, and this will be more noticeable when the number of models in each class is smaller, as it is the case for the order 2 of database indexing.

It is expected that improving the statistical significance of the inversions, by increasing the overall number of models in the database, will reduce the difference between non-indexed and indexed inversions. This well illustrated by Figure 7, which shows how the percentage of inverted models that preserve a given set of properties, in passing from non-indexed to indexed inversions, changes as a function of the size of the inversion database. For this figure, we have considered the two cases mentioned earlier: one where *all* values of the physical parameters of the model are exactly preserved by the indexing of the inversion database (star symbols), and the other where we look at the percentage of models where the inferred value of the magnetic strength is found to change by less than 20% (diamond symbols). The continuous (dashed) curve shows the case for the indexed inversion of order 1 (2). This figure summarizes the obvious fact that increasing the indexing order also increases the inversion error, because of the reduced number of database models falling in each class. At the same time, it also shows that, by increasing the number of models in the database, the inversion errors are also bound to decrease. For example, the trend shown in Figure 7 suggests that the errors on the inferred magnetic strength attained using a database with 1.2-1.3M models with an indexed inversion of order 2 should be comparable to the errors from an indexed inversion of order 1 over a database with only 0.25M models. These results indicate that the stability of the inversion results under indexing of the PCA database depends in fact on the density of the models in the database, although it changes rather slowly as a function of the total number of models.

It is legitimate to question whether the changes in the inferred values of the model parameters, which occur in passing from non-indexed to indexed inversions, may affect too large a portion of

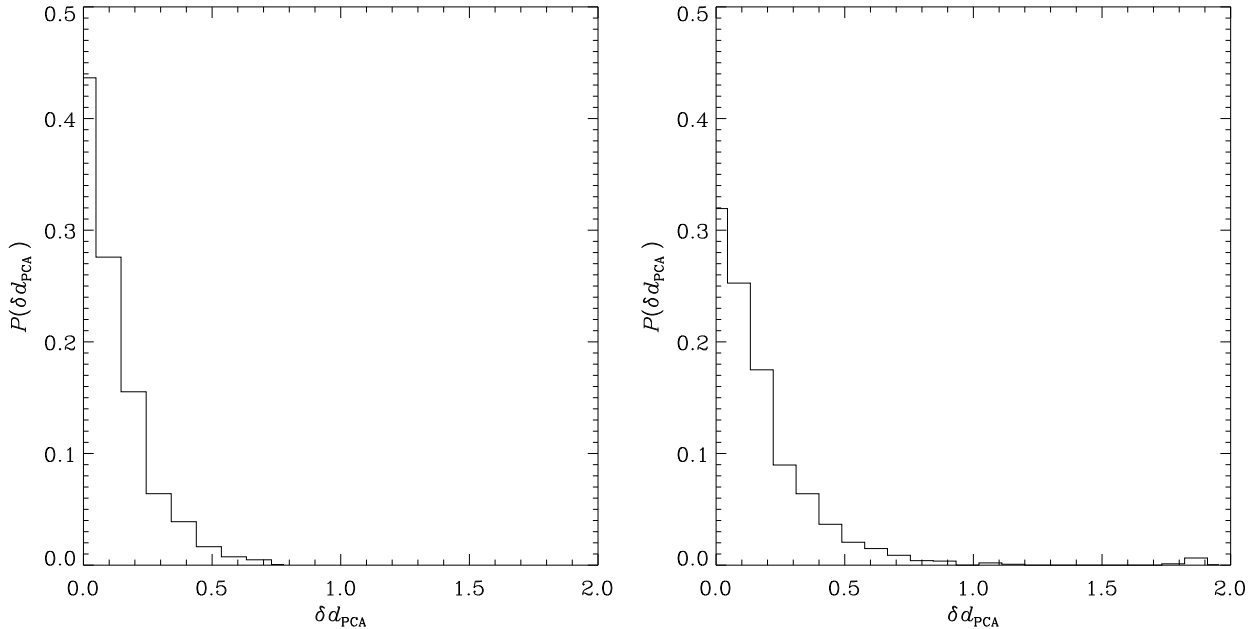


Fig. 8.— Normalized distributions of the relative change of the PCA distance, δd_{PCA} , for the indexed inversions of order 1 (left) and 2 (right). These distributions are calculated on the subset of map points for which the magnetic field strength is found to vary by more than 20% in passing from non-indexed to indexed inversions.

the map to justify the proposed method as a reliable approach to spectro-polarimetric inversion. On the other hand, the observed changes must be interpreted in the light of the possible presence of intrinsic ambiguities in the line formation model, which can result in very similar sets of emerging Stokes profiles even for magnetic configurations that may differ significantly. This fact is well illustrated by the distribution of δd_{PCA} for the set of map points where the inferred value of the magnetic field strength changes by more than 20% between non-indexed and indexed inversions (see also Figure 6). Figure 8 shows this (normalized) distribution for inversions based on the full databases of 0.75 million models. The left (right) panel shows the increase of the PCA distance for the indexed inversion of order 1 (2). The fact that this distribution gathers decidedly around zero, with 72% (62%) of the models showing less than a 20% increase in the PCA distance, statistically demonstrates that the changes in the inferred magnetic field caused by the indexing of the inversion databases has only a minor effect on the goodness of the profile fit, and that those changes are then compatible with the presence of intrinsic ambiguities of the line formation model.

The proposed method for the indexing of PCA inversion databases is particularly easy to implement. Along with the manifold increase in the inversion speed that is possible to attain, this is another attractive feature of the method. As it is apparent from comparing qualitatively the maps of Figure 5, as well as from the more detailed statistical analysis of the variations produced with different orders of indexing, which we presented above, the proposed method appears to be

adequate for fast handling of large synoptic datasets, such as those from full-disk observations of the Sun. Instruments such as the Synoptic Optical Long-term Investigations of the Sun (SOLIS) of the National Solar Observatory (Keller 1998), or the Chromosphere Magnetometer (ChroMag) of the High Altitude Observatory (De Wijn et al. 2012), currently under testing, can profit greatly from the proposed strategy of spectro-polarimetric inversion, and represent ideal testbeds of the method. Using a database with 0.5 million models, and an order of indexing of 2, it would take only about 30 minutes to fully invert an observation of the entire solar disk with a 1 arcsec spatial resolution.

On the other hand, the dramatic increase of the inversion speed granted by database indexing realistically opens to the possibility of using much larger PCA databases than in the past. This would allow to perform high-precision spectro-polarimetric inversions of smaller regions of the Sun, the typical size of a medium active region ($\sim 4 \text{ arcmin}^2$), using PCA databases with several tens of millions of models, for which the downsides of database indexing that we have previously discussed are expected to be significantly reduced. Another possible application of PCA indexed inversion is to provide a fast initialization of spectro-polarimetric inversions that rely on elaborate optimization schemes, such as the Levenberg-Marquardt algorithm (e.g., Asensio Ramos, Trujillo Bueno, & Landi Degl’Innocenti 2008), as an alternative to more cumbersome initialization methods such as those based on the genetic algorithm.

The authors thank the Kiepenheuer-Institut für Sonnenphysik for a grant of observing time that permitted the observations reported herein to be obtained. We also thank C. Beck, M. Collados, C. Kuckein, R. Rezeai, and W. Schmidt for assistance during the observing run, and C. Kuckein for assistance in data reduction. We thank HAO colleagues G. de Toma and A. Skumanich for a careful reading of the manuscript and for helpful comments. We are deeply indebted to the anonymous referee, who has done a very scrupulous job in reviewing the manuscript, and in suggesting clarifications and improvements to the original presentation of this work.

REFERENCES

- Asensio Ramos, A. 2012, ASP Conf. Ser. 463, The Second ATST-EAST Meeting: Magnetic Fields from the Photosphere to the Corona, eds. T. R. Rimmele, M. Collados Vera, et al. (ASP: San Francisco), 215
- Asensio Ramos, A., Trujillo Bueno, T., & Landi Degl’Innocenti 2008, ApJ, 683, 542
- Birkhoff, G., & S. Mac Lane 1953, A Survey of Modern Algebra, rev. ed. (MacMillan: New York)
- Casini, R. 2012, ASP Conf. Ser. 463, The Second ATST-EAST Meeting: Magnetic Fields from the Photosphere to the Corona, eds. T. R. Rimmele, M. Collados Vera, et al. (ASP: San Francisco), 193

- Casini, R., Bevilacqua, R., & López Ariste, A. 2005, *ApJ*, 622, 1265
- Casini, R., López Ariste, A., Tomczyk, S., & Lites, B. W. 2003, *ApJ*, 598, L67
- Collados, M., Lagg, A., Díaz García, J. J., Hernández Suárez, E., López López, R., Páez Mañá, E., Solanki, S. K. 2007, *ASP Conf. Ser.*, 368, *The Physics of Chromospheric Plasmas*, eds. P. Heinzel, I. Dorotovič, & R. J. Rutten (ASP: San Francisco), 611
- De Wijn, A. G., Bethge, C., Tomczyk, S., & McIntosh, S. 2012, *SPIE*, 8446, 78
- Eydenberg, M. S., Balasubramaniam, K. S., & López Ariste, A. 2005, *ApJ*, 619, 1167
- Jolliffe, I. T. 2002, *Principal Component Analysis*, 2nd ed. (Springer: New York)
- Keller, C. U. 1998, *SPIE*, 3352, 732
- Kuckein, C., Centeno Elliott, R., Martínez Pillet, V., Casini, R., Manso Sainz, R., & Shimizu, T. 2009, *A&A*, 501, 1113
- López Ariste, A., & Casini, R. 2002, *ApJ*, 575, 529
- López Ariste, A., & Casini, R. 2003, *ApJ*, 582, L51
- McKay, M. D., Beckman, R. J., & Conover, W. J. 1979, *Technometrics*, 21, 239
- Pearson, K. 1901, *Phil. Mag.*, 2, 559
- Press, W. H., Teukolsky, S. A., Vetterling, W. T., & Flannery, B. P. 2007, *Numerical Recipes: The Art of Scientific Computing*, 3rd ed. (Cambridge University: Cambridge)
- Rees, D. E., López Ariste, A., Thatcher, J., & Semel, M. 2000, *A&A*, 355, 759
- Rimmele, T., & the ATST Team 2008, *Adv. Sp. Res.*, 42, 78
- Skumanich, A. P., & López Ariste, A. 2002, *ApJ*, 570, 379
- Trujillo Bueno, J. 2010, *Recent Advances in Chromospheric and Coronal Polarization Diagnostics, in Magnetic Coupling between the Interior and Atmosphere of the Sun*, *Proc. Astrophysics and Space Science*, eds. S. S. Hasan & R. J. Rutten (Springer: Berlin), 118